High-Order Impedance Boundary Conditions for Multilayer Coated 3-D Objects

Olivier Marceaux and Bruno Stupfel

***Abstract*—The scattering problem by a multilayer coated three-dimensional (3-D) object where the coating is modeled by an impedance boundary condition (IBC) is considered. First, the exact boundary condition is obtained for an infinite planar coating with an arbitrary number of layers. Then, various approximations for the pseudodifferential operators involved in this exact condition are proposed. In the expressions of the resulting IBC's, all tangential derivatives of the fields of order higher than two are suppressed. These IBC's are compared, in terms of numerical efficiency, by computing either the reflection coefficients on an infinite planar metal-backed coating or the radar cross section (RCS) of a perfectly conducting coated sphere using the tangent plane approximation. In both cases, it is found that the highest order IBC models the coating with a good accuracy. Finally, some guidance is given on how this IBC may be numerically implemented in an integral equation or a finite-element formulation for an arbitrarily shaped object.**

***Index Terms*—Impedance boundary conditions, nonhomogeneous materials.**

I. Introduction

THE numerical solution of the scattering problem by a multilayer coated 3-D object can be significantly simplified if an impedance boundary condition (IBC) is used to model the behavior of the coating. Implemented, e.g., in an integral equation formulation defined on the outermost boundary of the coating [1], the IBC may lead to substantial savings in computing times and memory requirements since Maxwell's equations need not be solved in the inhomogeneous domain. An IBC relates the tangential components of the electric field $\underline{E}$ to those of the magnetic field $\underline{H}$ and constitutes a local, hence approximate, boundary condition. The simplest and most popular IBC is the Leontovich IBC (LIBC) [2]. However, it is known to be poorly efficient for, e.g., low index coatings [3]. Several improved IBC's have been proposed in the past [4]–[10] that increase the order of the tangential derivatives of $\underline{E}$ and/or $\underline{H}$ involved in the relationship, and have been obtained either in the space or in the spectral domain.

In the space domain, a generalized IBC (GIBC) was first proposed in [5] for two-dimensional (2-D) problems where the coefficients in the IBC were derived from the exact reflection coefficient calculated for a plane wave incident on an infinite planar surface. It was extended later on to three-dimensional (3-D) electromagnetic problems (see [8] and references included therein). The determination of the coefficients in the IBC from the exact reflection coefficient necessitates *ad hoc* complicated approximations that are difficult to apply to a multilayer coating. To date, no numerical implementation of the GIBC for the solution of a 3-D problem is known. In the spectral domain, a successful attempt to model bodies of revolution with a metal-backed layer has been presented in [7]. However, the application of this particular IBC to objects of general shape is not straightforward. Recently, an exact relationship between $\underline{E}$ and $\underline{H}$ has been obtained on the outer surface of a metal-backed layer from which an IBC that involves tangential derivatives of $\underline{H}$ only has been derived [9]. Applications of the spectral domain methodology to multiple layers have been discussed in [10].

The organization of this paper is as follows. First, we consider an infinite planar coating for which we derive in Section II the exact boundary condition in the space domain by employing the method proposed in [11] for 2-D problems. Section III is devoted to the derivation, from this exact relationship and, without loss of generality, when the coating is backed by a perfectly electric conducting (PEC) plane, of various IBC's which include most of the aforementioned ones. The order of the tangential derivatives of $\underline{E}$ and/or $\underline{H}$ that appear in the final expressions is at most equal to two in order to facilitate the numerical implementation of the resulting IBC in an integral equation (or a finite element) formulation. The numerical efficiency of these IBC's is evaluated by computing the corresponding reflection coefficients. In Section IV we investigate the performances of the IBC's for a perfectly conducting coated sphere, assuming that the terms involving the surface curvatures are negligible (tangent plane approximation). Finally, we indicate in Section V how these IBC's may be implemented in an integral equation (or finite element) formulation for an object of arbitrary shape.

II. Exact Boundary Conditions for an Infinite Planar Coating

We consider a stratified isotropic medium infinite in the x and y directions where each layer l is characterized by its thickness d_l, dielectric permittivity ϵ_l and magnetic permeability μ_l. The z axis is directed along the increasing values of l, and the assumed time dependence is $\exp(i\omega t)$. We show in the Appendix that the 3-D transpose of the 2-D methodology proposed in [11] for a

Manuscript received March 30, 1999; revised September 22, 1999. This work was performed during a trainee student period of O. Marceaux at CEA/CESTA from August to December 1997.

O. Marceaux is with COFRAMI, Espace Montaigne, St. Médard en Jalles, 33160 France.

B. Stupfel is with CEA/CESTA, Commissariat à l'Énergie Atomique, Le Barp, 33114 France.

Publisher Item Identifier S 0018-926X(00)01643-4.

metal-backed layer yields the following exact relationships in layer l, viz. $z_{l-1} \le z \le z_l = \sum_{j=1}^{l} d_j$

$$\begin{aligned}
&\underline{z} \times \underline{E}(z) \\
&\quad = \cos[k_l(z_l - z)\sqrt{1+t_l}] \left[\underline{z} \times \underline{E}(z_l) \right. \\
&\qquad \left. + \frac{i\eta_l}{k_l^2} \frac{\tan[k_l(z_l - z)\sqrt{1+t_l}]}{\sqrt{1+t_l}} \left(k_l^2 - L_R\right) \underline{H}_{\mathrm{tg}}(z_l) \right] \\
&\underline{H}_{\mathrm{tg}}(z) \\
&\quad = \cos[k_l(z_l - z)\sqrt{1+t_l}] \left[\underline{H}_{\mathrm{tg}}(z_l) \right. \\
&\qquad \left. + \frac{i}{\eta_l k_l^2} \frac{\tan[k_l(z_l - z)\sqrt{1+t_l}]}{\sqrt{1+t_l}} \left(k_l^2 + L_D\right) [\underline{z} \times \underline{E}(z_l)] \right]
\end{aligned} \tag{1}$$

$k_l = \omega\sqrt{\epsilon_l \mu_l}$, $\eta_l = \sqrt{\mu_l/\epsilon_l}$, $\underline{H}_{\mathrm{tg}} = -\underline{z} \times \underline{z} \times \underline{H}$, and the operators t_l, L_R, L_D are defined as

$$\begin{aligned}
t_l &= \nabla_{\mathrm{tg}}^2 / k_l^2 = \left(\partial_x^2 + \partial_y^2\right) / k_l^2 \\
L_R(\underline{V}) &= \underline{\nabla} \times \{\underline{z}(\underline{\nabla} \times \underline{V})_z\}, \quad L_D(\underline{V}) = \underline{\nabla}_{\mathrm{tg}}(\underline{\nabla} \cdot \underline{V}_{\mathrm{tg}})
\end{aligned} \tag{2}$$

$\underline{V}$ is an arbitrary vector in the (xy) plane and $\underline{\nabla} = \underline{x}\partial_x + \underline{y}\partial_y + \underline{z}\partial_z$. The pseudodifferential operators in (1) are defined by their Taylor series in z [see, e.g., definition (A.2) of $\cos[k_l(z_l - z)\sqrt{1+t_l}]$ in the Appendix]. If we let $z = z_{l-1}$ in (1), then we obtain the exact relationships that link the values of the fields on the inner and outer boundaries of layer l

$$\begin{aligned}
\underline{z} \times \underline{E}(z_{l-1}) &= \cos[k_l d_l \sqrt{1+t_l}] \left[\underline{z} \times \underline{E}(z_l) + T_R^l \underline{H}_{\mathrm{tg}}(z_l) \right] \\
\underline{H}_{\mathrm{tg}}(z_{l-1}) &= \cos[k_l d_l \sqrt{1+t_l}] \left[T_D^l [\underline{z} \times \underline{E}(z_l)] \right. \\
&\qquad \left. + \underline{H}_{\mathrm{tg}}(z_l) \right] \\
T_R^l &= \frac{i\eta_l}{k_l^2} P_l \left(k_l^2 - L_R\right) \\
T_D^l &= \frac{i}{\eta_l k_l^2} P_l \left(k_l^2 + L_D\right)
\end{aligned} \tag{3}$$

with

$$P_l = \frac{\tan[k_l d_l \sqrt{1+t_l}]}{\sqrt{1+t_l}}. \tag{4}$$

The first two equations in (3) can be conveniently written as

$$U^{l-1} = T^l U^l \tag{5a}$$

where $U^l = [z \times \underline{E}(z_l), \underline{H}_{\mathrm{tg}}(z_l)]^t$ (the superscript t denotes matrix transpose), and the transition matrix T^l is defined as

$$T^l = \cos[k_l d_l \sqrt{1+t_l}] \begin{pmatrix} 1 & T_R^l \\ T_D^l & 1 \end{pmatrix}. \tag{5b}$$

From (5a), we readily obtain the exact relationships that link the values of the fields on both sides of a medium with p layers

$$U^{l-1} = \left(\prod_{j=1}^{p} T^{l+j-1} \right) U^{l+p-1}. \tag{5c}$$

Now, we consider the case of a metal-backed medium. Let the half-space $z \le z_0$ be perfectly conducting. Then $z \times \underline{E}(z_0) = 0$ and, for one layer, we get from (5a)

$$\underline{z} \times \underline{E}(z_1) = -\frac{i\eta_1}{k_1^2} P_1 \left(k_1^2 - L_R\right) \underline{H}_{\mathrm{tg}}(z_1) \tag{6}$$

while, for two layers, we obtain from (5c) with $p = 2$

$$\begin{aligned}
&\left\{ 1 - \frac{\eta_1}{\eta_2 k_1^2 k_2^2} P_1 P_2 \left(k_1^2 - L_R\right) \left(k_2^2 + L_D\right) \right\} \underline{z} \times \underline{E}(z_2) \\
&\quad = -i \left\{ \frac{\eta_1}{k_1^2} P_1 \left(k_1^2 - L_R\right) + \frac{\eta_2}{k_2^2} P_2 \left(k_2^2 - L_R\right) \right\} \underline{H}_{\mathrm{tg}}(z_2)
\end{aligned} \tag{7}$$

Similar relationships can be easily derived from (5c) for an arbitrary number of layers. Note that (6) is the space domain transpose of [9, eq. (30)] that has been established in the spectral domain.

III. Derivation and Validation of the IBCs for a Metal-Backed Planar Coating

Without loss of generality, we consider in this section an infinite planar metal-backed coating. First, from the exact relationship in (6), we derive in Section III-A various IBC's for a monolayer coating. For reasons that will be explained in Section V, we drop in the expressions of these IBC's all tangential derivatives of $\underline{E}$ and $\underline{H}$ whose order is higher than two. Their numerical efficiencies are evaluated by computing the corresponding reflection coefficients for an incident plane wave. Then, in Section III-B, we proceed along the same lines for a two layers coating, while the evaluation of the performances of the corresponding IBC's is postponed to Section IV. Let us mention here that the methodology developed for two layers is easily applicable to a larger number of layers.

A. Monolayer Coating

A numerical implementation of the exact relationship in (6) is possible only if the pseudo-differential operator P_1 defined in (4) is approximated. For an incident plane wave $\exp[-i(k_{0x}x + k_{0y}y - k_0 z\cos\theta)]$ where $k_0 = 2\pi/\lambda_0$ is the free-space wave number, the field inside the coating is $\psi = Q\exp[-i(k_{0x}x + k_{0y}y - k_1 z\cos\theta_1)] + S\exp[-i(k_{0x}x + k_{0y}y + k_1 z\cos\theta_1)]$ with $\sin\theta_1 = \sin\theta/N_1$ where $N_l = \sqrt{\epsilon_l\mu_l/(\epsilon_0\mu_0)}$ is the optical index of layer l. We get from (2) $t_1\psi = -\psi(k_{0x}^2 + k_{0y}^2)/k_1^2 = -\psi\sin^2\theta/N_1^2$. Hence, in the spectral domain, $t_1 \to 0$ as $|N_1| \to \infty$. If we let $t_1 = 0$ in (4), then we obtain

$$P_1 = \tan(k_1 d_1). \tag{8}$$

Dropping all tangential derivatives of $\underline{H}_{\mathrm{tg}}$ in (6), we get the LIBC

$$\underline{z} \times \underline{E}(z_1) = -i\eta_1 \tan(k_1 d_1) \underline{H}_{\mathrm{tg}}(z_1) \tag{9}$$

(8) is exact in normal incidence $(\theta = 0)$ or in oblique incidence when $|N_1| \to \infty$. We choose to enforce this property to all of the approximations of P_l that will be subsequently derived.

Similarly to what has been done in [7] and [9], we approximate P_1 by a rational fraction of t_1, i.e., we let

$$P_1 = \frac{a_0 + a_1 t_1}{1 + b_1 t_1}. \tag{10}$$

Notice that the degrees of the polynomials in (10) are voluntarily restricted to one since the choice of higher degrees would induce tangential derivatives of the fields whose order is higher than two. If the Taylor series expansions in t_1 of P_1 and of the rational fraction are chosen to be identical at $t_1 = 0$ up to the second-order derivatives, then we get a $(1,1)$ Padé approximation of P_1 at $t_1 = 0$, and the values of the coefficients a_0, a_1, b_1 in (3) are

$$\begin{aligned} \text{Padé:}\quad a_0 &= \tan(k_1 d_1) \\ a_1 &= \frac{1 - 4k_1^2 d_1^2 - \cos(2k_1 d_1) + 2k_1 d_1 \tan(k_1 d_1)}{4[-2k_1 d_1 + \sin(2k_1 d_1)]} \\ b_1 &= \frac{-6k_1 d_1 + [3 + 4k_1^2 d_1^2 + 3\cos(2k_1 d_1)]\tan(k_1 d_1)}{4[-2k_1 d_1 + \sin(2k_1 d_1)]} \end{aligned} \tag{11}$$

An *a priori* less accurate approximation is the first-order Taylor approximation of P_1 at $t_1 = 0$, which yields

$$\begin{aligned} \text{Taylor:}\quad a_0 &= \tan(k_1 d_1) \\ a_1 &= \frac{k_1 d_1 - \tan(k_1 d_1) + k_1 d_1 \tan^2(k_1 d_1)}{2} \\ b_1 &= 0. \end{aligned} \tag{12}$$

Alternatively, we may enforce (10) at three values of t_1, namely $t_1 = 0$, $t_1 = \beta_1$, and $t_1 = \beta_2$, which gives (13), shown at the bottom of the page. Finally, inserting the approximation (10) of P_1 in (6) and multiplying (6) by $(1 + b_1 t_1)$, we get

$$\begin{aligned} &(1 + b_1 t_1)\underline{z} \times \underline{E}(z_1) \\ &\quad = -\frac{i\eta_1}{k_1^2}(a_0 + a_1 t_1)\left(k_1^2 - L_R\right)\underline{H}_{\text{tg}}(z_1). \end{aligned}$$

Noticing from the definitions in (2) that $t_1 = (L_D - L_R)/k_1^2$ and dropping in the above expression all tangential derivatives of $\underline{E}$ and $\underline{H}$ whose order is higher than two, we obtain

$$\begin{aligned} &\left[1 + b_1 \frac{L_D - L_R}{k_1^2}\right] \underline{z} \times \underline{E}(z_1) \\ &\quad = -i\eta_1 \left[a_0 + a_1 \frac{L_D}{k_1^2} - (a_0 + a_1)\frac{L_R}{k_1^2}\right] \underline{H}_{\text{tg}}(z_1). \end{aligned} \tag{14}$$

This IBC has the same form and involves the same operators than the high-order absorbing boundary condition (HOABC) devised in [12]. If the values of the coefficients in (14) are those given in (12), then we obtain the IBC defined by [9, eq. (35)] in which the tangential derivatives of $\underline{H}_{\text{tg}}$ of order higher than two are discarded. Also, it is important to note that the values of a_1 and b_1 in (13) when β_1 and β_2 tend to 0 are actually those of a_1 and b_1 in (11)

$$\begin{aligned} \lim_{\beta_1, \beta_2 \to 0} a_1(\text{collocation}) &= a_1(\text{Padé}) \\ \lim_{\beta_1, \beta_2 \to 0} b_1(\text{collocation}) &= b_1(\text{Padé}). \end{aligned} \tag{15}$$

We now proceed to the evaluation of the numerical efficiencies of the above IBC's by computing their respective reflection coefficients for a planar incident wave whose direction of incidence makes the angle θ with the z axis and for the two polarizations: TM ($\underline{H}$ orthogonal to $\underline{z}$) and TE ($\underline{E}$ orthogonal to $\underline{z}$). The exact reflection coefficients $r_{\text{TM}}^{\text{ex}}(\theta)$ and $r_{\text{TE}}^{\text{ex}}(\theta)$ are

$$\begin{aligned} r_{\text{TM}}^{\text{ex}}(\theta) &= \\ &\frac{-\cos\theta + i\eta_{1r}\sqrt{1 - \sin^2\theta/N_1^2}\,\tan\left\{k_1 d_1 \sqrt{1 - \sin^2\theta/N_1^2}\right\}}{\cos\theta + i\eta_{1r}\sqrt{1 - \sin^2\theta/N_1^2}\,\tan\left\{k_1 d_1 \sqrt{1 - \sin^2\theta/N_1^2}\right\}} \\ r_{\text{TE}}^{\text{ex}}(\theta) &= \\ &\frac{-\sqrt{1 - \sin^2\theta/N_1^2} + i\eta_{1r}\cos\theta\tan\left\{k_1 d_1 \sqrt{1 - \sin^2\theta/N_1^2}\right\}}{\sqrt{1 - \sin^2\theta/N_1^2} + i\eta_{1r}\cos\theta\tan\left\{k_1 d_1 \sqrt{1 - \sin^2\theta/N_1^2}\right\}} \end{aligned} \tag{16}$$

where $\eta_{lr} = \eta_l/\eta_0$. For the LIBC in (9) we find

$$\begin{aligned} r_{\text{TM}}(\theta) &= \frac{-\cos\theta + i\eta_{1r}\tan(k_1 d_1)}{\cos\theta + i\eta_{1r}\tan(k_1 d_1)} \\ r_{\text{TE}}(\theta) &= \frac{i\eta_{1r}\tan(k_1 d_1)\cos\theta - 1}{i\eta_{1r}\tan(k_1 d_1)\cos\theta + 1} \end{aligned} \tag{17}$$

while, for the IBC in (14), we get

$$\begin{aligned} r_{\text{TM}}(\theta) &= \frac{-\delta(\theta)\cos\theta + i\sigma_{\text{TM}}(\theta)}{\delta(\theta)\cos\theta + i\sigma_{\text{TM}}(\theta)} \\ r_{\text{TE}}(\theta) &= \frac{-\delta(\theta) + i\sigma_{\text{TE}}(\theta)\cos\theta}{\delta(\theta) + i\sigma_{\text{TE}}(\theta)\cos\theta} \end{aligned} \tag{18a}$$

with

$$\begin{aligned} \delta(\theta) &= 1 - b_1 \frac{\sin^2\theta}{N_1^2} \\ \sigma_{\text{TM}}(\theta) &= \eta_{1r}\left[a_0 - (a_0 + a_1)\frac{\sin^2\theta}{N_1^2}\right] \\ \sigma_{\text{TE}}(\theta) &= \eta_{1r}\left[a_0 - a_1 \frac{\sin^2\theta}{N_1^2}\right]. \end{aligned} \tag{18b}$$

$$\begin{aligned} \text{Collocation:}\quad a_0 &= \tan(k_1 d_1) \\ a_1 &= \frac{-\beta_2 P_1(\beta_2)(P_1(\beta_1) - a_0) + \beta_1 P_1(\beta_1)(P_1(\beta_2) - a_0)}{\beta_1\beta_2(P_1(\beta_1) - P_1(\beta_2))} \\ b_1 &= \frac{-\beta_2(P_1(\beta_1) - a_0) + \beta_1(P_1(\beta_2) - a_0)}{\beta_1\beta_2(P_1(\beta_1) - P_1(\beta_2))} \end{aligned} \tag{13}$$

The IBC's with the values of the coefficients given by (11), (12) and (13) are termed PIBC, TIBC, and CIBC, respectively. Regarding the CIBC, it has been found that the best results are obtained when the parameters β_1 and β_2 are such that

$$\beta_j = -\gamma_j^2/N_1^2, \quad 0 \le \gamma_j < 1, \quad j = 1, 2. \tag{19}$$

As a consequence, identity (15) is satisfied when $|N_1| \to \infty$. Troughout this paper, we chose $\gamma_1 = 0.5$ and $\gamma_2 = 0.9$. As a comparison, we have also calculated the reflection coefficients, as formulated in [8, eqs. (5.62)], that correspond to the second-order GIBC defined by [8, eqs. (5.63)] and subsequently termed GIBCSV. Fig. 1 plots the moduli of the various reflection coefficients versus θ for $\epsilon_1/\epsilon_0 = \mu_1/\mu_0 = N_1 = 2 - i/2$ and $k_0 d_1 = 0.15$. We note the poor performance of the LIBC in TM polarization due to the low value of $|N_1| = 2.06$ and the relative inefficiency of the GIBCSV around $\theta = 0$ for TE polarization, while the TIBC, PIBC, and CIBC are in excellent agreement with the exact results. To further investigate the behavior of the IBC's versus N_1 and d_1, we have computed the following average error

$$\mathrm{error}(N_1, d_1) = \log \left[\max_{j=\mathrm{TM,TE}} \int_0^{\pi/2} \left| r_j(\theta, N_1, d_1) - r_j^{\mathrm{ex}}(\theta, N_1, d_1) \right|^2 d\theta \right]$$

where r_j and r_j^{ex} denotes the IBC and exact reflection coefficient, respectively. In view of Fig. 2 that plots $\mathrm{error}(N_1, d_1)$ versus $|N_1|$ and d_1/λ_0 with $\mu_1 = \mu_0$, $\mathrm{Im}(N_1) = -0.1$, we may readily draw the following conclusions. First, as it has been already observed in Fig. 1, the LIBC and GIBCSV perform poorly. For this reason, we will discard the latter in the following, while keeping the former for the sake of comparison as it is the most popular. Second, the efficiency of the IBC's increases as $|N_1|$ increases. This is not surprising since the IBC's in (9) and (14) are constructed in such a way as to be exact when $|N_1| \to \infty$. Also, the PIBC and CIBC perform very similarly, on account of the choice of the coefficients β_1, β_2 in (19) and of the result stated in (15), and yield the best results. This was to be expected, since it is well known that a smooth function like P_1 in the vicinity of $t_1 = 0$ is more accurately approximated by a ratio of two polynomials of degree one in t_1, as in the PIBC and CIBC, than by a polynomial of the same degree as in the TIBC or of degree zero as in the LIBC. Third, for a fixed value of N_1, the accuracy of the IBCs decreases as d_1/λ_0 increases. The reason for this is the following. The coefficients in (10) are computed from a Taylor series expansion of P_1 at $t_1 = 0$ which, considering (4), necessarily involves the one of P_1'

$$P_1' = \tan[k_1 d_1 \sqrt{1+t_1}] = \tan\left[k_1 d_1 \left(1 + t_1/2 + O\left(t_1^2\right)\right)\right] = \frac{\tan(k_1 d_1) + \tan\left[k_1 d_1 t_1/2 + O\left(t_1^2\right)\right]}{1 - \tan(k_1 d_1)\tan\left[k_1 d_1 t_1/2 + O\left(t_1^2\right)\right]}.$$

As a consequence, the terms in the infinite Taylor series expansion of P_1' at $t_1 = 0$ contain powers of $\tan(k_1 d_1)$ and of $k_1 d_1$ that may not be negligible for large values of $k_1 d_1$. Actually, the ridges observed for the TIBC in Fig. 2, which correspond to a high level of error, are centered on the curves $|\tan(k_1 d_1)| = |\tan(2\pi N_1 d_1/\lambda_0)| = \infty$. In short, P_1 is a function of *two* variables, t_1 and $k_1 d_1$ and both should be considered, which is beyond the scope of this paper.

B. Two Layers Coating

Here, we have to approximate the exact relationship in (7). We choose to approximate P_1 and P_2 independently with the representations that have been proposed in Section III-A. This allows an easy derivation of the IBC's for a larger number of layers. The simplest approximation to (7) is obtained by letting $P_1 = \tan(k_1 d_1)$, $P_2 = \tan(k_2 d_2)$ and discarding all tangential derivatives of $\underline{z} \times \underline{E}$ and $\underline{H}_{\mathrm{tg}}$

$$\left[1 - \frac{\eta_1}{\eta_2}\tan(k_1 d_1)\tan(k_2 d_2)\right] \underline{z} \times \underline{E}(z_2) = -i[\eta_1 \tan(k_1 d_1) - \eta_2 \tan(k_2 d_2)]\underline{H}_{\mathrm{tg}}(z_2). \tag{20}$$

Alternatively, if we approximate P_1 and P_2 by rational fractions as in (10), viz.,

$$P_1 = \frac{a_{01} + a_{11} t_1}{1 + b_{11} t_1}, \quad P_2 = \frac{a_{02} + a_{12} t_2}{1 + b_{12} t_2} \tag{21}$$

and drop in the final result all tangential derivatives of order higher than two, then (7) yields the following generic form for the IBC

$$[C_1 + C_2 L_D - C_3 L_R]\underline{z} \times \underline{E}(z_2) = i[D_1 + D_2 L_D - D_3 L_R]\underline{H}_{\mathrm{tg}}(z_2) \tag{22}$$

with

$$\begin{aligned}
C_1 &= 1 - \frac{\eta_1}{\eta_2} a_{01} a_{02} \\
C_2 &= \frac{b_{11}}{k_1^2} + \frac{b_{12}}{k_2^2} - \frac{\eta_1}{\eta_2}\left[\frac{a_{11} a_{02}}{k_1^2} + \frac{a_{01}}{k_2^2}(a_{12} + a_{02})\right] \\
C_3 &= \frac{b_{11}}{k_1^2} + \frac{b_{12}}{k_2^2} - \frac{\eta_1}{\eta_2}\left[\frac{a_{01} a_{12}}{k_2^2} + \frac{a_{02}}{k_1^2}(a_{11} + a_{01})\right] \\
D_1 &= -\eta_1 a_{01} - \eta_2 a_{02} \\
D_2 &= -\eta_1\left[\frac{a_{11}}{k_1^2} + \frac{a_{01} b_{12}}{k_2^2}\right] - \eta_2\left[\frac{a_{21}}{k_2^2} + \frac{a_{02} b_{11}}{k_1^2}\right] \\
D_3 &= D_2 - \frac{\eta_1 a_{01}}{k_1^2} - \frac{\eta_2 a_{02}}{k_2^2}.
\end{aligned} \tag{23}$$

The coefficients a_{01}, a_{11}, b_{11} are equal to those in (11), (12) or (13), depending on the type of approximation that is employed, and the expressions of a_{02}, a_{12}, b_{12} are obtained from the same formulas by substituting subscript 2 to subscript 1. In a number of coatings, the index increases from the outer layer to the inner layer and, consequently, the angle of refraction decreases as one gets closer to the conducting surface. Consequently, it seems reasonable to think that such a coating will be satisfactorily modeled if the operator P_l corresponding to the outermost layer is approximated as in (10) while those related to the other layers

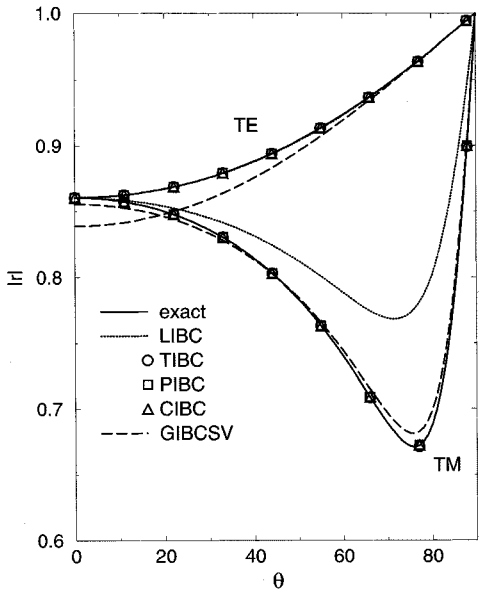

Fig. 1. Modulus of the exact and IBCs reflection coefficients versus θ.

are approximated as in (8). Proceeding as previously, we get (22) for a two layers coating with

$$C_1 = 1 - \frac{\eta_1}{\eta_2} a_{01} a_{02}, \quad C_2 = \frac{b_{12}}{k_2^2} - \frac{\eta_1 a_{01}}{\eta_2 k_2^2}(a_{12} + a_{02})$$
$$C_3 = \frac{b_{12}}{k_2^2} - \frac{\eta_1 a_{01} a_{12}}{\eta_2 k_2^2}$$
$$D_1 = -\eta_1 a_{01} - \eta_2 a_{02}, \quad D_2 = -\frac{1}{k_2^2}(\eta_1 a_{01} b_{12} + \eta_2 a_{21})$$
$$D_3 = D_2 - \frac{\eta_2 a_{02}}{k_2^2} \tag{24}$$

where the values of a_{02}, a_{12}, b_{12} remain unchanged and $a_{01} = \tan(k_1 d_1)$.

IV. Coated PEC Sphere

Here, we solve analytically the scattering problem by a sphere on the outermost boundary of which the various IBC's defined in the previous section are prescribed. This allows us to investigate their performances for a monolayer and a two layers coating, successively.

We consider a PEC sphere of radius R, illuminated by a plane wave $(\underline{E}^{\text{inc}}, \underline{H}^{\text{inc}})$. d is the thickness of the coating on the outermost boundary of which the IBC (22) is prescribed. Note that this formulation of the IBC obtained for two layers is general and includes formulations (9) and (14) established for one layer. In spherical coordinates the scattered field may be expressed for $r \geq R + d$ as

$$\underline{E}^s(\underline{r}) = -\sum_{n=0}^{\infty} f_n[\bar{a}_n \underline{\bar{M}}_{1n}(\underline{r}) + \bar{b}_n \underline{\bar{N}}_{1n}(\underline{r}) + n(n+1)(\bar{a}_n \underline{\bar{M}}_{-1n}(\underline{r}) - \bar{b}_n \underline{\bar{N}}_{-1n}(\underline{r}))]$$
$$\underline{H}^s(\underline{r}) = -i\sum_{n=0}^{\infty} f_n[\bar{b}_n \underline{\bar{M}}_{1n}(\underline{r}) + \bar{a}_n \underline{\bar{N}}_{1n}(\underline{r}) - n(n+1)(\bar{b}_n \underline{\bar{M}}_{-1n}(\underline{r}) - \bar{a}_n \underline{\bar{N}}_{-1n}(\underline{r}))]. \tag{25}$$

The notations are those defined in [12]. Substituting these forms of $\underline{E}^s, \underline{H}^s$ in (22) with $\underline{E} = \underline{E}^{\text{inc}} + \underline{E}^s$, $\underline{H} = \underline{H}^{\text{inc}} + \underline{H}^s$, we get after some algebra the following expressions for the coefficients $\bar{a}_n$ and $\bar{b}_n$:

$$\bar{a}_n = -\frac{\tilde{j}_n(x)}{\tilde{h}_n(x)} \times \frac{\left[D_1 - \frac{n(n+1)k_0^2}{x^2} D_2 + \frac{\eta_0 x j_n(x)}{\tilde{j}_n(x)}\left(C_1 - \frac{n(n+1)k_0^2}{x^2} C_2\right)\right]}{\left[D_1 - \frac{n(n+1)k_0^2}{x^2} D_2 + \frac{\eta_0 x h_n(x)}{\tilde{h}_n(x)}\left(C_1 - \frac{n(n+1)k_0^2}{x^2} C_2\right)\right]}$$
$$\bar{b}_n = -\frac{j_n(x)}{h_n(x)} \times \frac{\left[D_1 - \frac{n(n+1)k_0^2}{x^2} D_3 - \frac{\eta_0 \tilde{j}_n(x)}{x j_n(x)}\left(C_1 - \frac{n(n+1)k_0^2}{x^2} C_3\right)\right]}{\left[D_1 - \frac{n(n+1)k_0^2}{x^2} D_3 - \frac{\eta_0 \tilde{h}_n(x)}{x h_n(x)}\left(C_1 - \frac{n(n+1)k_0^2}{x^2} C_3\right)\right]},$$
$$x = k_0(R+d). \tag{26}$$

Employing (22) implies that the terms involving the surface curvatures are not taken into account and we refer to [7] for a discussion on the validity of this approximation. The bistatic radar cross section (RCS), defined at $\varphi = 0$ as $\text{RCS}(\theta) = 10\log(\sigma(\theta))$ with

$$\sigma(\theta) = \frac{4\pi}{k_0^2}\left|\sum_{n=1}^{\infty} \frac{(-1)^n(2n+1)}{n(n+1)}\left[\bar{a}_n \frac{P_n^1(\cos\theta)}{\sin\theta} - \bar{b}_n d_\theta P_n^1(\cos\theta)\right]\right|^2 : \text{TM}$$
$$= \frac{4\pi}{k_0^2}\left|\sum_{n=1}^{\infty} \frac{(-1)^n(2n+1)}{n(n+1)}\left[\bar{b}_n \frac{P_n^1(\cos\theta)}{\sin\theta} - \bar{a}_n d_\theta P_n^1(\cos\theta)\right]\right|^2 : \text{TE} \tag{27}$$

(P_n^1 is the Legendre function of orders 1 and n) is computed versus the observation angle θ using (26), and compared to the exact one, first for a monolayer and then for a double layer coating. $R = 1$ m in the numerical examples that follow.

The results displayed in Fig. 3 are obtained at $f = 2$ GHz for a dielectric layer of thickness $d = 2.5$ cm $= \lambda_0/6$ with relative permittivity $\epsilon_r = 1.2 - 0.5i$ and permeability $\mu_r = 1$. The values of the coefficients C_i, D_i in (26) are obtained by identifying (22) with (9) for the LIBC, or with (14) for the PIBC, TIBC and CIBC. For the latter we use (19) with $\gamma_1 = 0.5$, $\gamma_2 = 0.9$. As it has been already observed in Section III-A, the PIBC and CIBC yield the same results which are superimposed on the exact ones. We have actually verified in various numerical experiments that the CIBC, as defined by (13) and (19), performs very similarly to the PIBC. For this reason, we will consider only the latter in the following. On the other hand, on account of the low value of the index ($|N| = 1.14$), the error committed when employing the LIBC or the TIBC can be quite large. An other illustration of the efficiency of the PIBC is the following. Let us assume that we want to minimize the backscattered RCS of the sphere with a low index dielectric material. On account of Weston's theorem [16], one may think that this will

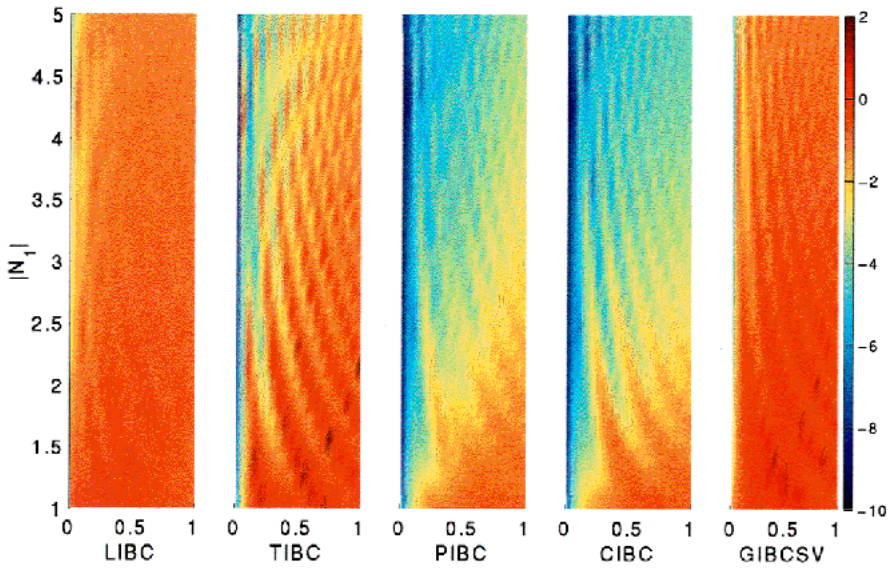

Fig. 2. *Error* versus $|N_1|$ and d_1/λ_0, $0 \leq d_1/\lambda_0 \leq 1$, with $\mu_1 = \mu_0$, $\mathrm{Im}(N_1) = -0.1$.

be achieved if the material is such that its relative impedance $Z = i\tan(k_0 dN)/N$ with $N = \sqrt{\epsilon_r}$ is equal to unity since a zero backscattered RCS is obtained if the LIBC is employed. For a given value of d, say $d = 3$ cm, the solution of equation $Z = 1$ with the lowest value of $|N|$ yields $\epsilon_r = 1.958135707 - 1.5163i$ ($|N| = 1.574$) at 2 GHz. Fig. 4 plots the exact RCS and the RCS computed with the LIBC and the PIBC. It demonstrates the high efficiency of the PIBC and shows that a low index material satisfying $Z = 1$ is less efficient for RCS reduction than a high index material with $Z = 1$ that will be correctly modeled by the LIBC.

Now, we consider a two layers dielectric coating of thickness $d = d_1 + d_2$. The calculation frequency is 2 GHz and the parameters of the coating are $d_1 = 1.5$ cm $= \lambda_0/10$, $\epsilon_{r1} = 1.8 - i$ for the inner layer ($|N_1| = 2.06$), and $d_2 = 2.5$ cm $= \lambda_0/6$, $\epsilon_{r2} = 1.2 - 0.5i$ for the outer layer ($|N_2| = 1.14$). The bistatic RCS is calculated with the LIBC (20) and the IBC defined as in (22) and (23) where the values of the coefficients in (23) correspond either to the Padé or to the Taylor approximation employed for both layers. These IBC's are termed PPIBC and TTIBC, respectively. In addition, since the index increases when going inwards, we have computed the RCS with the LIBC for the inner layer and the PIBC for the outer one. The corresponding values of the coefficients in (22) are those given in (24) and the resulting IBC is termed LPIBC. The results displayed in Fig. 5 emphasize, once again, the superior efficiency of the Padé approximation over the other ones. Also, we note that for this particular coating the LPIBC and the PPIBC yield very similar results. We may further observe, by comparing Figs. 5 and 3, that these IBC's are less accurate for a two layers coating than for a monolayer coating. Considering, e.g., the PPIBC, the reason for this is the following. Although the operators P_1 and P_2 in the exact relationship (7) are approximated by the rational fractions defined in (21) and, consequently, induce high-order tangential derivatives of the fields in the IBC, more of these derivatives are dropped in the final derivation of the IBC for two layers than

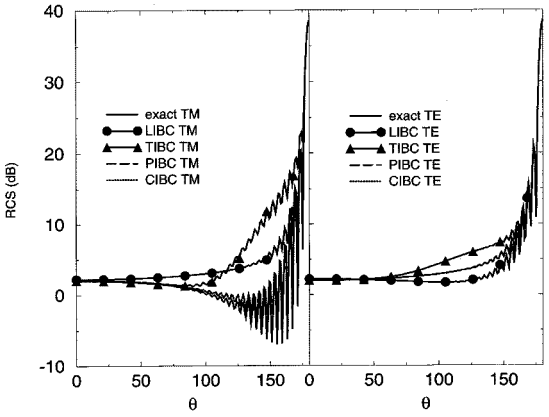

Fig. 3. Bistatic RCS versus θ for the monolayer PEC sphere.

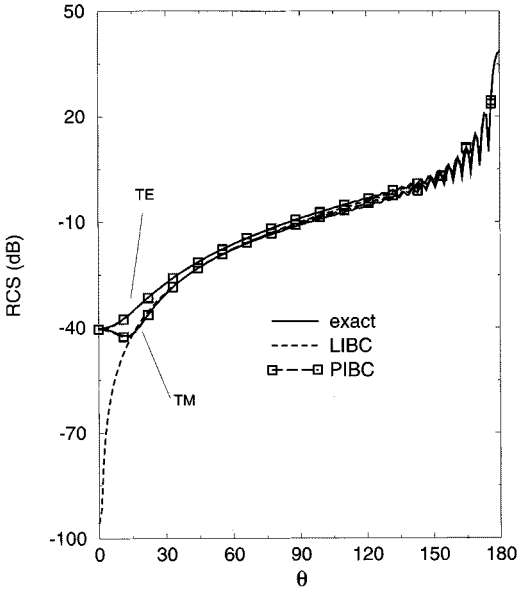

Fig. 4. Bistatic RCS versus θ for the monolayer PEC sphere with $Z = 1$.

for one layer, on account of the self-imposed constraint that all derivatives of order higher than two must be suppressed.

V. Numerical Implementation of the IBC's

We investigate in this section how the generic expression of the high-order IBC defined by (22) can be numerically implemented in an integral equation (IE), or a finite-element (FE), formulation for an arbitrarily shaped object. If an IE is employed to solve the scattering problem, then we may proceed as in [7], viz. the combined field integral equation (CFIE) [13] is implemented on the outermost surface of the coating, and (22) provides the additional equations that permit to solve the problem. Alternatively, we may model some part of the coating with a FE formulation and use (22) to represent the remaining part. In both cases, we consider the following variational formulation derived from (22)

$$\int_S \underline{G}\cdot[C_1 + C_2 L_D - C_3 L_R]\underline{n}\times\underline{E}\,dS = i\int_S \underline{G}\cdot[D_1 + D_2 L_D - D_3 L_R]\underline{H}_{\rm tg}\,dS \qquad (28)$$

where $\underline{n}$ designates the outward normal to the surface S where the IBC is prescribed and $\underline{G}$ is a test vector. Integration by parts yields

$$\int_S \{C_1\underline{G}_{\rm tg}\cdot(\underline{n}\times\underline{E}) - C_2\underline{\nabla}\cdot\underline{G}_{\rm tg}[\underline{\nabla}\cdot(\underline{n}\times\underline{E})] - C_3(\underline{\nabla}\times\underline{G})_n(\underline{\nabla}\times(\underline{n}\times\underline{E}))_n\}\,dS = i\int_S \{D_1\underline{G}_{\rm tg}\cdot\underline{H}_{\rm tg} - D_2\underline{\nabla}\cdot\underline{G}_{\rm tg}[\underline{\nabla}\cdot\underline{H}_{\rm tg}] - D_3(\underline{\nabla}\times\underline{G})_n(\underline{\nabla}\times\underline{H})_n\}\,dS. \qquad (29)$$

Let us consider first the FE formulation where we assume, without loss of generality, that the unknown is the magnetic field $\underline{H}$. The corresponding variational formulation applied to the computational domain exterior to S involves a surface integral on S of $\underline{K} = \underline{n}\times\underline{E}$ (see, e.g., [12]). If this domain is meshed with tetrahedrons and the standard first-order edge-based functions [14] are employed, then we use these same functions to represent $\underline{G}$ and $\underline{K}$ on S. Furthermore, to discretize the surface divergence terms $\underline{\nabla}\cdot\underline{G}_{\rm tg}$, $\underline{\nabla}\cdot\underline{K}$, and $\underline{\nabla}\cdot\underline{H}_{\rm tg}$ in (29), we use the technique indicated in [12]. As a result, we obtain from (29) the linear system of equations $M_K K = M_H H$ where the matrices M_K and M_H are symmetric.

Conversely, if the problem is solved by employing the CFIE, then the unknowns are $\underline{K}$ and $\underline{J} = \underline{n}\times\underline{H}$ defined on S. We assume that S is meshed with triangles. A possibility is to represent $\underline{K}$, $\underline{J}$, and $\underline{G}$ ($\underline{G}$ is now a vector tangent to S) by the standard Rao–Wilson–Glisson (RWG) basis functions [15]. We substitute $-\underline{n}\times\underline{J}$ to $\underline{H}_{\rm tg}$ in (28), use the identities $L_R(\underline{n}\times\underline{J}) = -\underline{n}\times L_D(\underline{J})$, $L_D(\underline{n}\times\underline{J}) = -\underline{n}\times L_R(\underline{J})$ [12], and integrate by parts to get

$$\int_S \{C_1\underline{G}\cdot\underline{K} - C_2(\underline{\nabla}\cdot\underline{G})(\underline{\nabla}\cdot\underline{K}) - C_3(\underline{\nabla}\times\underline{G})_n(\underline{\nabla}\times\underline{K})_n\}\,dS = i\int_S \{D_1(\underline{n}\times\underline{G})\cdot\underline{J} - D_2(\underline{\nabla}\times(\underline{n}\times\underline{G}))_n(\underline{\nabla}\times\underline{J})_n - D_3[\underline{\nabla}\cdot(\underline{n}\times\underline{G})](\underline{\nabla}\cdot\underline{J})\}\,dS$$

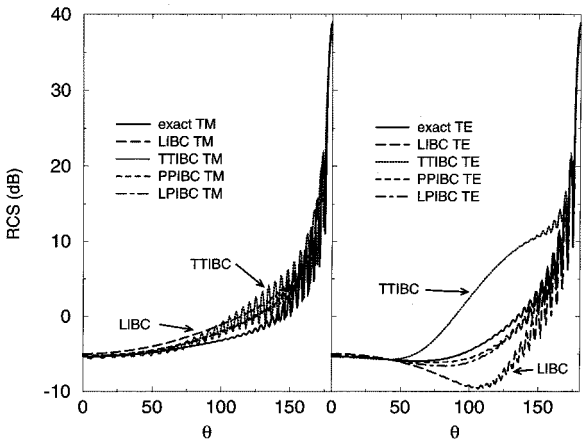

Fig. 5. Bistatic RCS versus θ for the two layers PEC sphere.

$$= i\int_S \{D_1(\underline{n}\times\underline{G})\cdot\underline{J} - D_2(\underline{\nabla}\cdot\underline{G})(\underline{\nabla}\times\underline{J})_n + D_3(\underline{\nabla}\times\underline{G})_n(\underline{\nabla}\cdot\underline{J})\}\,dS.$$

This time, the difficulty consists in discretizing the terms $(\underline{\nabla}\times\underline{G})_n$, $(\underline{\nabla}\times\underline{K})_n$, and $(\underline{\nabla}\times\underline{J})_n$. Again, we may use a similar technique to the one proposed in [12] to finally get $M'_K K = M_J J$ where the matrix M'_K is symmetric.

It is important to note at this point that the introduction in (22) of tangential derivatives whose order is higher than two would imply the use of higher order basis functions and complicate severely the special treatment needed for the correct discretization of the surface divergence terms (FE formulation) or of the curl terms (IE formulation).

VI. Conclusion

In this paper, we have derived an exact boundary condition for an infinite planar coating with an arbitrary number of layers that involves pseudodifferential operators. Various approximations for these operators have been proposed with the following constraints: 1) they must be exact in normal incidence or when the index of the material tends to infinity and 2) the order of the tangential derivatives of the fields that appear in the final expressions of the IBC's must be at most equal to two in order to facilitate their numerical implementation. Notice that the derivation of IBC's involving higher order tangential derivatives is straightforward. For a metal-backed layer, we have demonstrated the superior performances of the Padé and collocation approximations over the standard LIBC, as well as over the GIBC presented in [8], when the thickness of the coating is not too large in terms of the wavelength. Also, we have shown that a Taylor approximation may yield poor results. We have proceeded along the same lines for a double layer coating, and the methodology developed to this end is easily applicable to a larger number of layers, especially when the index increases from the outer layer to the inner layer. The numerical evaluation of the IBC's performances when implemented on a perfectly conducting coated sphere using the tangent plane approximation yields the same conclusions than those previously derived for the planar case. It is well known (see, e.g., [7], [12]) that this approximation is all the more justified as the radii of curvature are large compared to the

wavelength. More generally, the computation of the reflection coefficients for a planar surface, as given in (16)–(18b), or of the RCS of the coated sphere [(26), (27)], may serve in practical applications to determine the limitations of the various IBCs derived in Section III. Finally, we have pointed out some guidances on how the generic expression of the high-order IBC may be numerically implemented in an integral equation or a finite-element formulation for an arbitrarily shaped object, while employing standard first-order RWG or edge-based functions for the surface or volume unknowns, respectively.

APPENDIX

Here, we establish (1) by extending to the 3-D case the 2-D technique presented in [11] for a metal-backed layer. In layer l ($z_{l-1} \leq z \leq z_l$), we represent $E_x(z)$ by its Taylor Series expansion

$$E_x(z) = \sum_{n=0}^{\infty} \frac{(z-z_l)^{2n}}{(2n)!} \partial_z^{2n} E_x(z_l) + \sum_{n=0}^{\infty} \frac{(z-z_l)^{2n+1}}{(2n+1)!} \partial_z^{2n+1} E_x(z_l). \quad \text{(A.1)}$$

The Cartesian components of $\underline{E}$ satisfy the Helmholtz equation in medium l. Hence, $\partial_z^2 E_x(z) = -(k_l^2 + \nabla_{\text{tg}}^2) E_x(z)$, and $\partial_z^{2n} E_x(z) = (-1)^n (k_l^2 + \nabla_{\text{tg}}^2)^n E_x(z)$. Consequently

$$\sum_{n=0}^{\infty} \frac{(z-z_l)^{2n}}{(2n)!} \partial_z^{2n} E_x(z_l) = \cos[k_l (z_l - z)\sqrt{1+t_l}] E_x(z_l). \quad \text{(A.2)}$$

Also, we have $\partial_z^{2n+1} E_x(z) = (-1)^n (k_l^2 + \nabla_{\text{tg}}^2)^n \partial_z E_x(z)$ and, from Maxwell's equations, $\partial_z E_x(z) = -i(\partial_{yz}^2 H_z(z) - \partial_z^2 H_y(z))/(\omega \epsilon_l)$. Because $H_y(z)$ satisfies Helmholtz equation and $\underline{\nabla} \cdot \underline{H} = 0$, we get $\partial_z E_x(z) = -i(k_l^2 H_y(z) - \partial_{xy}^2 H_x(z) + \partial_x^2 H_y(z))/(\omega \epsilon_l)$. Hence

$$\sum_{n=0}^{\infty} \frac{(z-z_l)^{2n+1}}{(2n+1)!} \partial_z^{2n+1} E_x(z_l) = \frac{i}{\omega \epsilon_l k_l} \frac{\sin[k_l (z_l - z)\sqrt{1+t_l}]}{\sqrt{1+t_l}} \times \left[k_l^2 H_y - \partial_{xy}^2 H_x + \partial_x^2 H_y\right](z_l). \quad \text{(A.3)}$$

Finally, inserting (A.2) and (A.3) in (A.1), we obtain

$$E_x(z) = \cos[k_l (z_l - z)\sqrt{1+t_l}] E_x(z_l) + \frac{i}{\omega \epsilon_l k_l} \frac{\sin[k_l (z_l - z)\sqrt{1+t_l}]}{\sqrt{1+t_l}} \times \left[k_l^2 H_y - \partial_{xy}^2 H_x + \partial_x^2 H_y\right](z_l). \quad \text{(A.4)}$$

Similarly, we obtain for $E_y(z)$

$$E_y(z) = \cos[k_l (z_l - z)\sqrt{1+t_l}] E_y(z_l) - \frac{i}{\omega \epsilon_l k_l} \frac{\sin[k_l (z_l - z)\sqrt{1+t_l}]}{\sqrt{1+t_l}} \times \left[k_l^2 H_x - \partial_{xy}^2 H_y + \partial_y^2 H_x\right](z_l). \quad \text{(A.5)}$$

The first equation in (1) is the compact vector form of (A.4) and (A.5). Following along the same lines, we derive the second equation in (3).

REFERENCES

[1] L. N. Medgyesi-Mitschang and J. M. Putnam, "Integral equation formulations for imperfectly conducting scatterers," *IEEE Trans. Antennas Propagat.*, vol. AP-33, pp. 206–214, 1985.

[2] M. Leontovich, *Investigation on Radiowave Propagation—Part II*, Moscow, USSR: Academy of Sciences, 1948.

[3] D. S. Wang, "Limits and validity of the impedance boundary conditions on penetrable surfaces," *IEEE Trans. Antennas Propagat.*, vol. AP-35, pp. 453–457, 1987.

[4] S. M. Rytov, "Calcul du skin-effect par la méthode des perturbations," *J. Phys. USSR*, vol. 2, pp. 233–242, Oct. 1940.

[5] S. N. Karp and F. C. Karal Jr., "Generalized impedance boundary conditions with applications to surface wave structures," in *Electromagnetic Wave Theory*, J. Brown, Ed. New York: Pergamon, 1967, pt. 1, pp. 479–483.

[6] D. J. Hoppe and Y. Rahmat-Samii, "Scattering by superquadric dielectric-coated cylinders using higher order impedance boundary conditions," *IEEE Trans. Antennas Propagat.*, vol. 42, pp. 1600–1611, 1994.

[7] ——, "High order impedance boundary condition applied to scattering by coated bodies of revolution," *IEEE Trans. Antennas Propagat.*, vol. 40, pp. 1513–1523, 1992.

[8] T. B. A. Senior and J. L. Volakis, "Approximate boundary conditions in electromagnetics," *Inst. Elect. Eng. Electromagn. Waves Series 41*, 1995.

[9] R. Cicchetti, "A class of exact and higher-order surface boundary conditions for layered structures," *IEEE Trans. Antennas Propagat.*, vol. 44, pp. 249–259, 1996.

[10] D. J. Hoppe and Y. Rahmat-Samii, *Impedance Boundary Conditions in Electromagnetics*. Bristol, PA: Taylor Francis, 1995.

[11] J. M. Bernard, "Diffraction by a metallic wedge covered with a dielectric material," *Wave Motion*, vol. 9, pp. 543–561, 1987.

[12] B. Stupfel and M. Mognot, "Implementation and derivation of conformal absorbing boundary conditions for the vector wave equation," *J. Electromagn. Waves Applicat.*, vol. 12, pp. 1653–1677, 1998.

[13] J. R. Mautz and R. F. Harrington, "H-field, E-field, and combined field solutions for conducting bodies of revolution," *AEU*, vol. 32, pp. 156–164, 1978.

[14] J. C. Nédélec, "Mixed finite elements in R^3," *Numerische Math.*, vol. 35, pp. 315–341, 1980.

[15] S. M. Rao, D. R. Wilton, and A. W. Glisson, "Electromagnetic scattering by surfaces of arbitrary shape," *IEEE Trans. Antennas Propagat.*, vol. AP-30, pp. 409–418, 1982.

[16] V. H. Weston, "Theory of absorbers in scattering," *IEEE Trans. Antennas Propagat.*, vol. AP-11, pp. 578–584, Sept. 1963.

Olivier Marceaux received the Diplôme d'Ingénieur degree from the École Nationale Supérieure d'Électronique et de Radioélectricité de Bordeaux, France, in 1998.

He joined COFRAMI in November 1998.

Bruno Stupfel received the Diplôme d'Ingénieur degree from the École des Mines de Nancy, France, in 1977, and the Ph.D. degree in solid-state physics from the University of Strasbourg, France, in 1980.

From 1980 to 1982, he was with the Division Tubes Électroniques of Thomson-CSF where he worked on the development of traveling wave tubes. From 1982 to 1988 he was with the Acoustics Laboratory, Institut Supérieur d'Électronique du Nord, France, where he worked on integral equation methods and on the finite-element modeling of hydrophones. In 1988 he joined the Commissariat à l'Énergie Atomique, first at the CEL-V, France, where he was engaged in the development of computer codes and, since 1996, at the CESTA, France. During the academic year 1993-1994, he was a Visiting Scholar at the Electromagnetic Communication Laboratory, University of Illinois at Urbana-Champaign. His research interests include numerical methods in electromagnetics.